



Mixture unified gradient theory: a consistent approach for mechanics of nanobars

S. Ali Faghidian¹ · Krzysztof Kamil Żur² · Timon Rabczuk³

Received: 29 August 2022 / Accepted: 10 October 2022 / Published online: 22 October 2022
© The Author(s), under exclusive licence to Springer-Verlag GmbH, DE part of Springer Nature 2022

Abstract

The mixture unified gradient theory of elasticity is invoked for the meticulous assessment of peculiar size-dependent behavior of materials with nano-structural features. The size-dependency of the strain gradient theory and the stress gradient theory is consistently integrated with the classical continuum theory within a variational elasticity framework. The boundary-value problem associated with the dynamics of the nano-scale elastic bar is determined and enriched with the proper form of the extra non-standard boundary conditions. The constitutive model of the resultant fields is cast as differential relations in view of the stationarity of the proposed functional. The efficacy of the established generalized continuum theory in the accurate description of the size-effects at the ultra-small scale is put into evidence via electrostatic and elastodynamic analysis of nanobars. The nanoscopic characteristics of the wave dispersion are analytically addressed and appropriately compared with the counterpart experimental measurements. The elastostatic size-dependent behavior of nanobars is rigorously examined by applying an efficacious solution approach. Size-dependent elastostatic response of nanobars with kinematic constraints of interest in nano-mechanics are analytically determined and graphically illustrated. A promising approach to tackling the statics and dynamics of structural bar-type modules of advanced nano-systems is introduced.

Keywords Stationary variational principle · Nanobar · Wave dispersion · Elastostatic analysis · Stress gradient theory · Strain gradient theory · Size effects · Analytical modeling

1 Introduction

Materials with nano-structural features are extensively applied in advanced industries owing to their significantly enhanced physical characteristics. As the key elements of a broad spectrum of pioneering engineering systems, including MEMS and NEMS, investigation on the physical behavior of nano-structured materials attracted considerable attention [1–4]. Intricacy of performing experiments at the ultra-small scale and the high computational cost of

accomplishing atomistic-based numerical simulations, make them undesirable methodologies to capture the size-effects. On the contrary, hopes are anchored on the generalized continuum mechanics for nanoscopic study of the field quantities at the micro-/nano-scale where the classical continuum mechanics ceases to hold [5].

To realize the peculiar physical response of nano-structured materials at the ultra-small scale, the description of the constitutive law should be enriched via incorporation of the suitable characteristic length-scale parameters. Various forms of the generalized continuum theory, in essence, fall under the classifications of the higher-order grade continua and the nonlocal continua. Within the context of the higher-order grade continuum mechanics, additional gradients of the field variables are supplied in the kinematics or kinetics of the continua for each material point, correspondingly leads to the strain gradient theory [6, 7] or the stress gradient theory [8, 9]. As the strain gradient theory can effectively predict the stiffening phenomenon in nano-structures, implementation of the stress gradient theory yields the softening behavior of continua with nano-structural features. The

✉ S. Ali Faghidian
faghidian@gmail.com; faghidian@srbiau.ac.ir

✉ Krzysztof Kamil Żur
k.zur@pb.edu.pl

¹ Department of Mechanical Engineering, Science and Research Branch, Islamic Azad University, Tehran, Iran

² Faculty of Mechanical Engineering, Białystok University of Technology, Białystok, Poland

³ Institute of Structural Mechanics, Bauhaus-Universität Weimar, Marienstr. 15, 99423 Weimar, Germany

well-posedness of the gradient-type elasticity problems is broadly addressed in the literature for various nano-sized structures; nevertheless, let us restrict ourselves to mentioning some representative contributions [10–15]. As an utterly different school of thought, the kinetic field variables within the framework of the nonlocal continuum mechanics, are assumed to depend on the kinematic field variables of the reference point along with the nearby points of the continua [16]. As a result of intrinsic simplicity of the nonlocal elasticity theory, the pertinent literature amounts to a vast collection; some recent contributions are addressed in [17–23]. The nano-structured continua may demonstrate both the softening and stiffening size-effects contingent on the specific state conditions of the problem. Indeed, the higher-order grade continuum mechanics and the nonlocal elasticity theory cannot solely realize all the peculiar size-dependent characteristics of continua with nano-structural features. Unification of the generalized continuum theories to cover the wide spectrum of physical characteristics at the ultra-small scale attracted a significant amount of attention. A range of unified size-dependent continuum theories has, accordingly, merged in the literature; such as the nonlocal strain gradient model [24, 25], the nonlocal modified gradient theory [26, 27], the higher-order nonlocal gradient theory [28–30], the nonlocal surface elasticity [31, 32], and the mixture stress gradient theory [33]. Among this line of thought, the nonlocal strain gradient theory has stimulated interest in the literature and widely implemented to address the size-effects in nano-structures; to mention a few representative works refer to [34–40].

An essential insight into the peculiar size-dependent physics of elastic nanobars is provided in this study and a consistent approach for a rigorous assessment of size-effects is offered. The mixture unified gradient theory of elasticity is invoked for the nanoscopic study of the field quantities. Within the framework of the mixture unified gradient theory, size-dependency of the strain gradient theory and the stress gradient theory is consistently integrated with the classical continuum theory. A promising approach for accurate description of the behavior of continua with nano-structures is, therefore, presented. All the governing equations, i.e. the differential condition of dynamic equilibrium, classical and extra non-standard boundary conditions along with the constitutive laws of the resultant fields, are integrated into a single functional. Furthermore, the extra non-standard boundary conditions, needed to close the corresponding boundary-value problem on finite domains, are properly introduced and explicitly determined. A variety of generalized continuum theories of the gradient type are, also, retrieved by suitably driving the characteristic length-scale parameters. Efficacy of the conceived mixture unified gradient elasticity framework in addressing the peculiar features

of nanoscopic structures is evinced via thoroughly examining both the elastostatic and elastodynamic responses of nano-sized bars. A practical methodology for inverse determination of the characteristic length-scale parameters associated with the generalized continuum mechanics theories is, also, introduced.

The present study proceeds as follows; a stationary variational framework, founded on ad hoc functional space of kinetic source fields, is established in Sect. 2. The differential and a complete set of boundary conditions of equilibrium along with the constitutive laws of the resultant fields are determined. Nanoscopic characteristics of the wave dispersion is analytically addressed and numerically illustrated in Sect. 3. Section 3 is, moreover, enriched via comparing the dispersive behavior of waves detected within the established size-dependent continuum framework and the counterpart experimental measurements. Section 4 is devoted to rigorously examine the elastostatic response of nano-sized bars where a viable approach, based on successive integration of differential equations of lower-order, is applied to derive the analytical solution. To further enhance Sect. 4, nanoscopic elastostatic features of nano-sized bars with kinematic constraints of interest in nano-mechanics are numerically determined, graphically demonstrated, and thoroughly commented upon. Section 5 summarizes the study and presents the conclusion.

2 Mixture unified gradient elasticity for nanobar

To establish the variational framework consistent with the mixture unified gradient elasticity theory, the reference is made to an elastic thin bar of length L with cross-sectional area A . The material is characterized by the elastic modulus E and the material density ρ . The bar is referred to orthogonal Cartesian co-ordinates (x, y, z) , with the x abscissa coinciding with the centroidal axis of the bar and (y, z) defines the cross-section plane. The bar is considered to be subject to a generalized axial load \bar{f} , comprising the inertia forces, and the terminal loads, if any. Assuming the elastic bar to be sufficiently slender, the effects of the lateral deformation can be overlooked [41], and hence, the displacement field (u_x, u_y, u_z) writes as:

$$u_x = u(x, t), \quad u_y = 0, \quad u_z = 0, \quad (1)$$

where u denoting the axial displacement of the bar along the abscissa x at the time t . The kinematically compatible strain field consistent with the thin bar model, therefore, reads:

$$\varepsilon(x, t) = \partial_x u(x, t), \quad (2)$$

where ε representing the axial strain field. To consistently integrate the size-effects of the strain gradient theory, the stress gradient theory, and the classical elasticity, the stationary functional \mathbb{F} associated with the mixture unified gradient theory is introduced as:

$$\mathbb{F} = \int_0^L \left(N_0(x, t) \partial_x u(x, t) + N_1(x, t) \partial_{xx} u(x, t) - \bar{f}(x) u(x, t) - \frac{1}{2EA} (N_0(x, t))^2 - \frac{c^2}{2EA} (\partial_x N_0(x, t))^2 - \frac{1}{2EA(\mathfrak{M}c^2 + \ell^2)} (N_1(x, t))^2 - \frac{c^2}{2EA(\mathfrak{M}c^2 + \ell^2)} (\partial_x N_1(x, t))^2 \right) dx, \tag{3}$$

where the axial resultant fields N_0, N_1 are defined as the dual mathematical objects of the classical strain field $\varepsilon = \partial_x u$ and of its derivative along the bar longitudinal axis $\partial_x \varepsilon = \partial_{xx} u$. The significance of the strain gradient theory and the stress gradient theory is, respectively, addressed by the strain gradient characteristic length ℓ and the stress gradient length-scale parameter c . The mixture parameter is denoted by $0 \leq \mathfrak{M} \leq 1$ addressing the influence of the classical elasticity theory.

As it is well-established within the framework of stationary variational principles, the kinematic and kinetic field variables are selected as the primary variables subject to variation. The virtual kinetic source field variables are, moreover, assumed to have compact support on the bar domain. The first variation of the functional \mathbb{F} , following the integration by parts, writes as:

$$\delta \mathbb{F} = \int_0^L \left(\left(-\partial_x N_0(x, t) + \partial_{xx} N_1(x, t) - \bar{f}(x) \right) \delta u(x, t) - \delta N_0 \left(\partial_x u(x, t) - \frac{1}{EA} N_0(x, t) + \frac{c^2}{EA} \partial_{xx} N_0(x, t) \right) - \delta N_1 \left(\partial_{xx} u(x, t) - \frac{1}{EA(\mathfrak{M}c^2 + \ell^2)} N_1(x, t) + \frac{c^2}{EA(\mathfrak{M}c^2 + \ell^2)} \partial_{xx} N_1(x, t) \right) \right) dx + \left(N_0(x, t) - \partial_x N_1(x, t) \right) \delta u \Big|_0^L + N_1(x, t) \partial_x \delta u \Big|_0^L, \tag{4}$$

where the boundary congruence conditions are released in view of the heuristic assumption on the virtual kinetic source field to have compact support on the bar domain.

The differential and boundary conditions of equilibrium for a mixture unified gradient elastic bar are accordingly detected, imposing the stationarity of the functional $\delta \mathbb{F} = 0$, as:

$$\begin{aligned} \partial_x N_0(x, t) - \partial_{xx} N_1(x, t) + f(x) &= \rho A \partial_{tt} u(x, t), \\ (N_0(x, t) - \partial_x N_1(x, t)) \delta u \Big|_0^L &= 0, \\ N_1(x, t) \Big|_0^L &= 0, \end{aligned} \tag{5}$$

where the axial strains on the bar ends are assumed to have arbitrarily variations. The differential condition of dynamic equilibrium is notably obtained via implementation of the d'Alembert principle. As a choice normally preferred within the context of the generalized continuum mechanics, the axial force field N is introduced as:

$$N(x, t) = N_0(x, t) - \partial_x N_1(x, t). \tag{6}$$

The boundary-value problem of the dynamic equilibrium of the mixture unified gradient elastic bar is, therefore, simplified as:

$$\begin{aligned} \partial_x N(x, t) + f(x) &= \rho A \partial_{tt} u(x, t), \\ N(x, t) \delta u \Big|_0^L &= 0, \\ N_1(x, t) \Big|_0^L &= 0. \end{aligned} \tag{7}$$

The established differential condition of equilibrium is notably equipped with classical boundary conditions along with extra non-standard boundary conditions described in terms of the axial resultant field N_1 . The well-recognized privilege of application of stationary variational principles lies on properly detecting the constitutive model. The axial resultant fields N_0, N_1 , accordingly, are cast as ordinary differential relations expressed by:

$$\begin{aligned}
 N_0(x, t) - c^2 \partial_{xx} N_0(x, t) &= EA \partial_x u(x, t), \\
 N_1(x, t) - c^2 \partial_{xx} N_1(x, t) &= EA (\mathfrak{M}c^2 + \ell^2) \partial_{xx} u(x, t),
 \end{aligned} \tag{8}$$

determined by prescribing the stationarity of the introduced functional $\delta \mathbb{F} = 0$. The sought constitutive law of the axial force field is also determined, by virtue of the constitutive relations of N_0, N_1 along with the definition of N , as:

$$N(x, t) - c^2 \partial_{xx} N(x, t) = EA (\partial_x u(x, t) - (\mathfrak{M}c^2 + \ell^2) \partial_{xxx} u(x, t)). \tag{9}$$

The detected constitutive model of the axial resultant fields is properly enriched with the strain gradient characteristic length ℓ and the stress gradient length-scale parameter c incorporating the size-effects of the corresponding gradient theory of elasticity. Influence of the classical elasticity theory is, furthermore, integrated via the mixture parameter \mathfrak{M} . A promising methodology to capture the size-effects, capable of accurate realization of the physical characteristics of nano-sized elastic bars, is accordingly introduced. A close examination of the detected constitutive model reveals that the axial resultant fields are of higher-order than the counterpart classical resultants. As a result, to appropriately close the boundary-value problem on bounded domains, the explicit mathematical formula of the axial resultant field N_1 should be determined. Following some straightforward mathematics, it may be shown that the sought formula of N_1 can be cast in the form:

$$N_1(x, t) = \frac{c^2 (\mathfrak{M}c^2 + \ell^2)}{(1 - \alpha)c^2 - \ell^2} \left(\rho A \partial_t u(x, t) - q(x) - EA \left(\frac{\mathfrak{M}c^2 + \ell^2}{c^2} \right) \partial_{xx} u(x, t) \right). \tag{10}$$

Different forms of the generalized continuum theories of the gradient-type are recovered via appropriately driving the characteristic length-scale parameters. Setting the mixture parameter zero $\mathfrak{M} \rightarrow 0$ in Eq. (9), the constitutive law of the axial force within the context of the unified gradient theory of elasticity can be retrieved [24]:

$$N(x, t) - c^2 \partial_{xx} N(x, t) = EA (\partial_x u(x, t) - \ell^2 \partial_{xxx} u(x, t)). \tag{11}$$

As the strain gradient characteristic length tends to zero $\ell \rightarrow 0$ in Eq. (11), one get the stress gradient constitutive model of the axial force field as [9]:

$$N(x, t) - c^2 \partial_{xx} N(x, t) = EA \partial_x u(x, t). \tag{12}$$

Likewise, the strain gradient constitutive law of N can be retrieved as the stress gradient length-scale parameter vanishes $c \rightarrow 0$ in Eq. (11) [7]:

$$N(x, t) = EA (\partial_x u(x, t) - \ell^2 \partial_{xxx} u(x, t)). \tag{13}$$

In the absence of the strain gradient characteristic length ℓ in Eq. (9), the constitutive law of the axial force consistent with the mixture stress gradient theory can be restored as [33]:

$$N(x, t) - c^2 \partial_{xx} N(x, t) = EA (\partial_x u(x, t) - \mathfrak{M}c^2 \partial_{xxx} u(x, t)). \tag{14}$$

Lastly, the classical constitutive law of the axial force field can be retrieved via either vanishing the gradient length-scale parameters for a fixed mixture parameter $c, \ell \rightarrow 0$ or by setting the mixture parameter to unity in the absence of the strain gradient characteristic length $\mathfrak{M} \rightarrow 1, \ell \rightarrow 0$.

Noteworthy, the alternative approach to capture the softening structural response is to apply the nonlocal integral model within the context of the nonlocal strain gradient theory. Implementation of the nonlocal strain gradient theory is, nevertheless, restricted to some special nonlocal kernel functions [26–30]. In contrast to the nonlocal strain gradient framework, the reinstatement of the nonlocal integral convolution with the nonlocal differential model is no longer required in the proposed size-dependent continuum theory. The extra non-standard boundary conditions are explicitly determined in terms of the axial resultant fields without the requirement of utilizing the equivalence lemma indispensable within the context of the nonlocal gradient theory. The established variational framework of the mixture unified gradient elasticity can advantageously expose the peculiar size-dependent structural features of nanobars as put into

evidence by analytically examining both the elastostatic and elastodynamic responses of nano-sized elastic bars.

3 Wave dispersion characteristics

The classical elasticity theory is well-known to cease to hold in describing the dispersive behaviors of waves with wavelengths at the ultra-small scale. Restoring to generalized continuum mechanics is, therefore, foreseeable [30, 42]. Efficacy of the established mixture unified gradient theory of elasticity in proper determination of the dispersive characteristics of waves, as wavelength decreases, is evinced here.

To study the harmonic longitudinal waves dispersing along the longitudinal axis of the elastic nanobar, the axial force field is first determined in term of the kinematic field variables. By virtue of the differential condition of dynamic equilibrium Eq. (7) in the absence of the axially distributed load, the constitutive law of the axial force field is cast in the form of:

$$N(x, t) = \rho A c^2 \partial_{xxx} u(x, t) + EA \partial_x u(x, t) - EA (\mathfrak{M} c^2 + \ell^2) \partial_{xxx} u(x, t). \tag{15}$$

The differential condition governing the wave dispersion in the elastic nano-sized bar within the context of the mixture unified gradient theory is, subsequently, expressed as:

$$\rho A c^2 \partial_{xxx} u(x, t) - \rho A \partial_{tt} u(x, t) + EA \partial_{xx} u(x, t) - EA (\mathfrak{M} c^2 + \ell^2) \partial_{xxx} u(x, t) = 0. \tag{16}$$

The boundary conditions at infinity is tacitly fulfilled as the dispersive behavior of waves is examined on unbounded domains. For steady waves disperse in an infinitely extended homogeneous nano-sized elastic bar, the corresponding solution can be written as:

$$u(x, t) = \mathbb{U} \exp i(\kappa x - \omega t), \tag{17}$$

where $i = \sqrt{-1}$, κ denotes the wave number, ω represents the wave frequency, and \mathbb{U} indicates the wave amplitude, respectively. Substitution of the wave solution in the differential condition governing the wave dispersion within the context of the mixture unified gradient theory yields the sought phase velocity of axial waves $v = \omega/\kappa$ as:

$$v = \sqrt{\frac{E}{\rho}} \sqrt{\frac{1 + \kappa^2 (\mathfrak{M} c^2 + \ell^2)}{1 + c^2 \kappa^2}}. \tag{18}$$

To demonstrate the efficiency of the mixture unified gradient theory in predicting the peculiar dispersive behavior of axial waves at the nano-scale, let us examine the

experimental measurement of Silicon crystal for nanoscopic wavelengths as reported in [43]. The physical properties of Silicon crystal, as referenced in [44], is employed here. The detected closed-form analytical solution of the phase velocity of dispersive waves can be advantageously utilized to calibrate the characteristic length-scale parameters associated with the generalized continuum mechanics theories via applying the inverse theory approach. Accordingly, the discrepancy between the inversely determined phase velocity and the limited experimental measurements is minimized utilizing a nonlinear least square optimization procedure [45, 46].

The angular frequency in terms of the wave number of Silicon crystal, inversely determined in accordance with the mixture unified gradient theory, is illustrated in Fig. 1 in comparison with the experimental measurements. Applying the inverse theory methodology, the calibrated characteristic length-scale parameters associated with the mixture unified gradient theory are determined as $c = 8.54857 \times 10^{-2} \text{nm}$, $\ell = 0.26178 \times 10^{-2} \text{nm}$ and $\mathfrak{M} = 0.11512$. As noticeably observed in the comparison made in Fig. 1, the wave dispersion characteristics of Silicon crystal is realized on the entire domain with an excellent accuracy. The proposed mixture unified gradient theory can capture all the qualitative aspects of the experimental measurements at the nano-scale, and accordingly, provides a promising approach to precisely describe the size-dependent wave dispersion phenomenon at the ultra-small scale.

Nano-scale effect of the characteristic length-scale parameters on the dispersive behavior of axial waves is depicted as well. The non-dimensional form of the stress gradient

Fig. 1 Comparison of the wave dispersion in silicon crystal by experimental measurements [43] and the mixture unified gradient theory

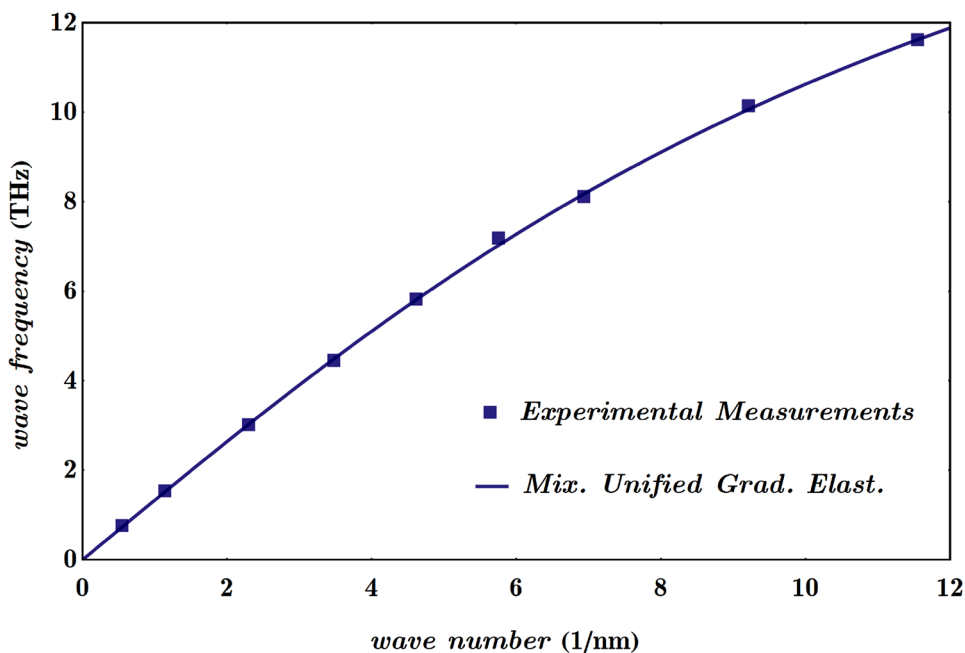


Fig. 2 Wave dispersion by mixture unified gradient theory: effects of the strain gradient parameter on the phase velocity

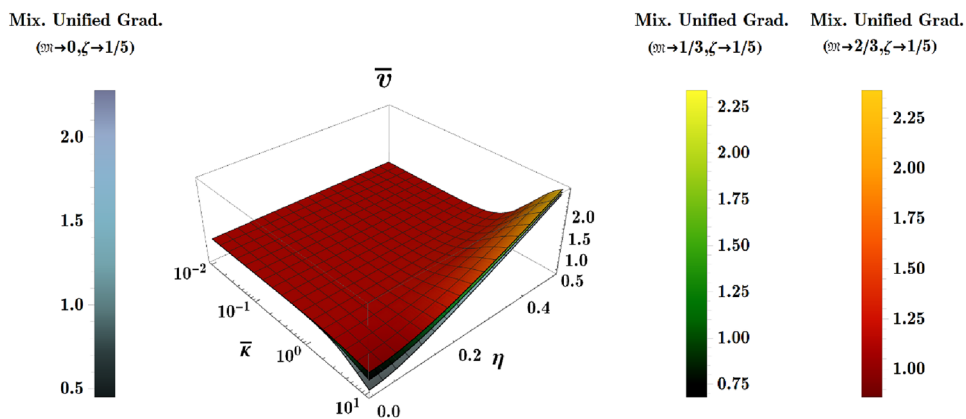
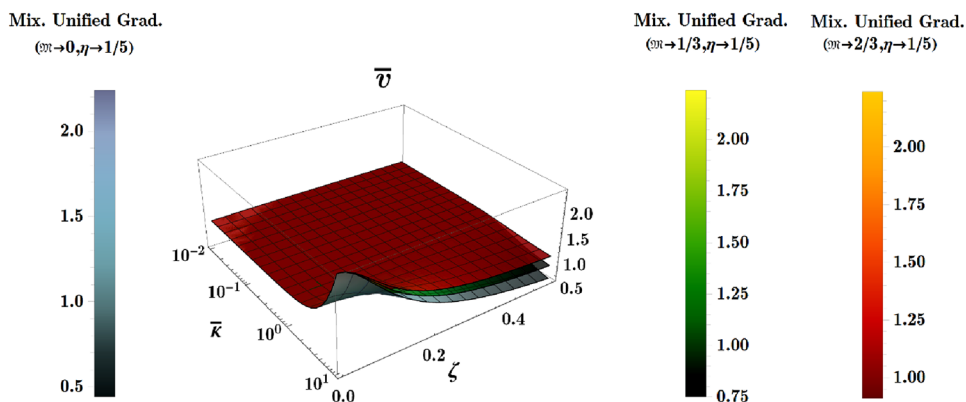


Fig. 3 Wave dispersion by mixture unified gradient theory: effects of the stress gradient parameter on the phase velocity



characteristic parameter ζ , the strain gradient characteristic parameter η , the wave number \bar{k} , and the phase velocity \bar{v} are introduced, for the sake of consistency, as:

$$\zeta = \frac{c}{L}, \eta = \frac{\ell}{L}, \bar{k} = \kappa L, \bar{v} = v \sqrt{\frac{\rho}{E}}. \tag{19}$$

Three-dimensional variation of the phase velocity of axial waves versus the characteristic length-scale parameters and the logarithmic scaling of the non-dimensional wave number is studied. Influence of the strain gradient and the stress gradient characteristic parameters on the dispersion of axial waves is, respectively, demonstrated in Figs. 2 and 3. The strain gradient characteristic parameter is assumed to range in the interval $[0, 1/2]$ in Fig. 2 as three values of the mixture parameter $\mathfrak{M} = 0, 1/3, 2/3$ are utilized for a prescribed value of the stress gradient characteristic parameter $\zeta = 1/5$. Likewise, as the stress gradient characteristic parameter is ranging in the interval $[0, 1/2]$ in Fig. 3, three values of the mixture parameter $\mathfrak{M} = 0, 1/3, 2/3$ are prescribed for a fixed strain gradient characteristic parameter $\eta = 1/5$. The (logarithm of) non-dimensional wave number [47] is

ranging in the interval $[10^{-2}, 10^{+1}]$ in the ensuing numerical illustrations.

As deducible from the presented illustrations, the strain gradient characteristic parameter η has the effect of increasing the phase velocity, and, therefore, a stiffening structural response in terms of the strain gradient characteristic parameter is realized. Otherwise, the softening structural response in terms of the stress gradient characteristic parameter ζ is demonstrated since the phase velocity of dispersive waves decreases with increasing the stress gradient characteristic parameter. As the mixture parameter \mathfrak{M} varies from 0 to 1, effects of the stress gradient theory in the constitutive model is continuously replaced with the influence of the classical elasticity theory. The phase velocity of axial waves increases with increasing the mixture parameter \mathfrak{M} , and accordingly, the stiffening structural response is revealed. The phase velocity of axial waves consistent with the mixture unified gradient theory remains unaltered for low wave numbers; the size-effect phenomenon is merely enhanced at higher wave numbers. This issue is expectedly occurred in consideration of the distinct nano-structural characteristics for sufficiently small wavelengths corresponding to large wave numbers.

4 Elastostatic characteristics of nanobars

To examine the elastostatic characteristics of nanobars, the axial deformation of a mixture unified gradient elastic bar with kinematic constraints of nano-mechanics interest is analytically addressed. In preference to directly solving the governing equation in terms of the axial displacement field, an efficacious approach based on integration of the differential equations of lower-order is utilized which can advantageously provide the exact analytical solutions [29, 48].

Integration of the differential condition of equilibrium Eq. (7), in the absence of the inertia forces, results in the equilibrated axial force N as:

$$N(x) = - \int_0^x f(\xi)d\xi + \mathfrak{A}_1, \tag{20}$$

where \mathfrak{A}_1 denotes the unknown integration constant. The axial displacement function u is afterward determined up to integration constants $\mathfrak{A}_2, \mathfrak{A}_3, \mathfrak{A}_4$ via solving the constitutive differential law Eq. (9) as:

$$\begin{aligned}
 u(x) = & \mathfrak{A}_2 \exp\left(\frac{x}{\sqrt{\mathfrak{M}c^2 + \ell^2}}\right) + \mathfrak{A}_3 \exp\left(-\frac{x}{\sqrt{\mathfrak{M}c^2 + \ell^2}}\right) + \mathfrak{A}_4 \\
 & + \frac{1}{2EA\sqrt{\mathfrak{M}c^2 + \ell^2}} \int_0^x \int_0^\xi \exp\left(\frac{\lambda - \xi}{\sqrt{\mathfrak{M}c^2 + \ell^2}}\right) (N(\lambda) - c^2 \partial_{\lambda\lambda} N(\lambda)) d\lambda d\xi \\
 & - \frac{1}{2EA\sqrt{\mathfrak{M}c^2 + \ell^2}} \int_0^x \int_0^\xi \exp\left(\frac{\xi - \mu}{\sqrt{\mathfrak{M}c^2 + \ell^2}}\right) (N(\mu) - c^2 \partial_{\mu\mu} N(\mu)) d\mu d\xi.
 \end{aligned} \tag{21}$$

The detected axial displacement field of the mixture unified gradient elastic bar should fulfill the classical and the extra non-standard boundary conditions as Eq (7). Prescribing the aforementioned set of boundary conditions, the unknown integration constants $\mathfrak{A}_1, \dots, \mathfrak{A}_4$ are determined, and consequently, the analytical solution of the axial displacement field of the nano-sized elastic bar is derived.

Let us assume the elastic nanobar to be subjected to the uniformly distributed axial load of intensity \bar{f} . For an elastic nano-sized bar consistent with the mixture unified gradient theory with fixed-ends, the classical kinematic boundary conditions consist of vanishing the axial displacement at both ends and the extra non-standard boundary conditions involve setting zero the axial resultant field N_1 at the bar ends. Following the proposed analytical solution approach,

the axial displacement of the uniformly loaded nanobar with fixed-ends is determined as:

$$\begin{aligned}
 u(x) = & \frac{\bar{f}}{EA} \left((-\ell^2 + \frac{1}{2}(L-x)x - c^2(-1 + \mathfrak{M})) \right. \\
 & \left. + (\ell^2 + c^2(-1 + \mathfrak{M})) \cosh\left(\frac{L-2x}{2\sqrt{\mathfrak{M}c^2 + \ell^2}}\right) \operatorname{sech}\left(\frac{L}{2\sqrt{\mathfrak{M}c^2 + \ell^2}}\right) \right).
 \end{aligned} \tag{22}$$

The maximum axial displacement is determined for numerical illustrations as:

$$\begin{aligned}
 u_{\max} = & \frac{\bar{f}}{8EA} (-8\ell^2 + L^2 - 8c^2(-1 + \mathfrak{M}) + 8(\ell^2 + c^2(-1 + \mathfrak{M})) \operatorname{sech} \\
 & \left(\frac{L}{2\sqrt{\mathfrak{M}c^2 + \ell^2}} \right)).
 \end{aligned} \tag{23}$$

Likewise, the classical boundary conditions of an elastic nanobar with fixed-free ends include vanishing the axial displacement and the axial force field at the fixed and free ends, respectively. The mixture unified gradient elastic bar with fixed-free ends is, furthermore, subject to the same extra non-standard boundary conditions, i.e. vanishing the

axial resultant field N_1 at both ends. Implementation of the introduced analytical solution approach yields the axial displacement of the uniformly loaded nanobar with fixed-free ends as:

$$\begin{aligned}
 u(x) = & \frac{\bar{f}}{EA} \left((-\ell^2 + Lx - \frac{1}{2}x^2 - c^2(-1 + \mathfrak{M})) \right. \\
 & \left. + (\ell^2 + c^2(-1 + \mathfrak{M})) \cosh\left(\frac{L-2x}{2\sqrt{\mathfrak{M}c^2 + \ell^2}}\right) \operatorname{sech}\left(\frac{L}{2\sqrt{\mathfrak{M}c^2 + \ell^2}}\right) \right).
 \end{aligned} \tag{24}$$

The maximum axial displacement of a uniformly loaded nano-sized bar within the context of the mixture unified gradient theory is, nevertheless, insensitive to the characteristic length-scale parameters. For the sake of numerical illustrations, the axial displacement field at the mid-span of the mixture unified gradient elastic bar is determined and employed:

$$u_{x=L/2} = \frac{\bar{f}}{8EA} \left(-8\ell^2 + 3L^2 - 8c^2(-1 + \mathfrak{M}) + 8(\ell^2 + c^2(-1 + \mathfrak{M})) \operatorname{sech} \left(\frac{L}{2\sqrt{\mathfrak{M}c^2 + \ell^2}} \right) \right). \tag{25}$$

The addressed analytical solutions of the displacement field of the mixture unified gradient elastic bar can efficiently incorporate the size-effect phenomenon at the ultra-small scale. It is of notice that the erroneous inference, preceded in literature, is stemmed from prescribing the imprecise form of the extra non-standard boundary conditions [41]. The subsequent non-dimensional axial displacement function \bar{u} is, furthermore, introduced for the sake of consistency:

$$\bar{u} = \frac{EA}{fL^2} u. \tag{26}$$

Nanoscopic influence of the characteristic length-scale parameters on the elastostatic characteristics of nanobars is examined here. The non-dimensional axial deformation of the nano-sized elastic bar at the mid-span is normalized with respect to the corresponding results of the classical bar model \bar{u}_0 . Three-dimensional variation of the normalized axial deformation function of the mixture unified gradient

elastic bar is depicted in Figs. 4 and 5, respectively, for fixed-end and fixed-free boundary conditions. As the stress gradient and the strain gradient characteristic parameters range in the interval $[0, 1/2]$, three values of the mixture parameter $\mathfrak{M} = 0, 1/3, 2/3$ are prescribed.

Taking into consideration the numerical results illustrated in Figs. 4 and 5, it is noticeably observed that the established mixture unified gradient theory of elasticity reveals a softening structural response in terms of the stress gradient characteristic parameter ζ , i.e. a larger ζ involves a larger axial displacement for prescribed values of \mathfrak{M}, η . The axial deformation field of the nano-scale elastic bar decreases as the strain gradient characteristic parameter η increases, and, therefore, the mixture unified gradient theory exposes a stiffening structural response in terms of the strain gradient characteristic parameter for given values of \mathfrak{M}, ζ . With varying the mixture parameter from 0 to 1, the effects of the stress gradient theory are reinstated with those of the classical elasticity theory. The axial displacement of the mixture unified gradient elastic bar, accordingly, decreases with increasing the mixture parameter for prescribed values of ζ, η . A stiffening structural response in terms of the mixture parameter is, accordingly, confirmed. The expected nanoscopic features of the elastostatic axial deformation of

Fig. 4 Maximum axial deformation of the mixture unified gradient nanobar with fixed-end boundary conditions

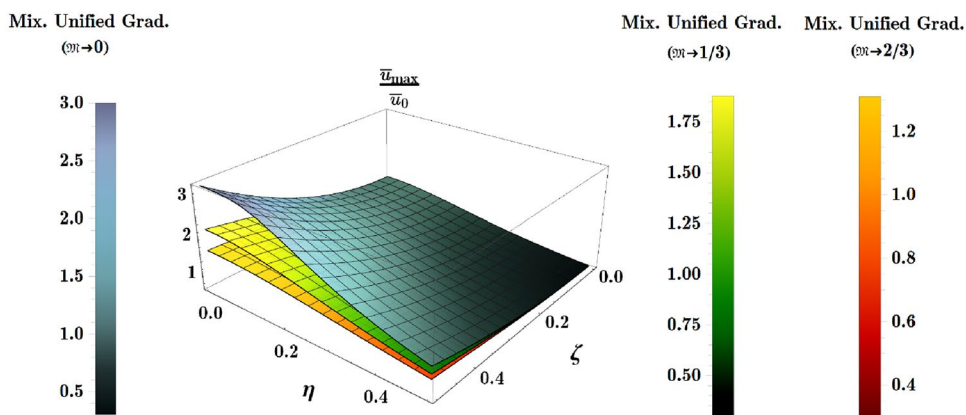


Fig. 5 Midspan axial deformation of the mixture unified gradient nanobar with fixed-free boundary conditions

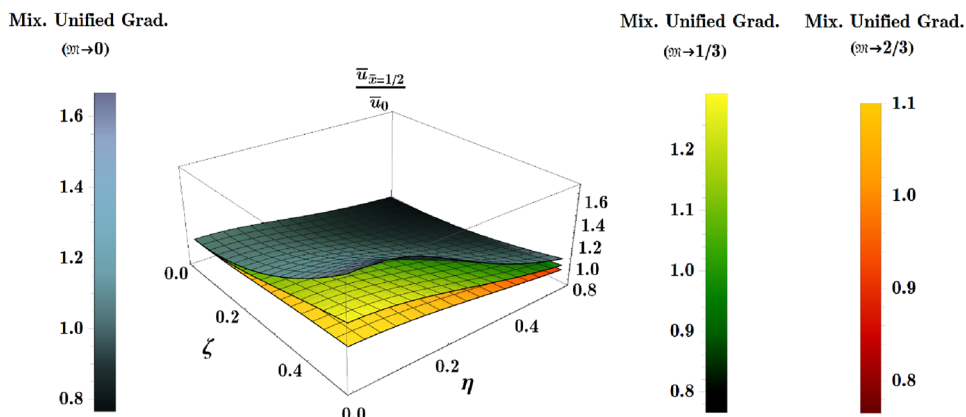


Table 1 Normalized maximum axial deformation of a mixture unified gradient elastic nanobar with fixed-ends

\bar{u}_{\max}/\bar{u}_0												
ζ	$\mathfrak{M} \rightarrow 0$						$\mathfrak{M} \rightarrow 1/3$					
	$\eta=0$	$\eta=0.1$	$\eta=0.2$	$\eta=0.3$	$\eta=0.4$	$\eta=0.5$	$\eta=0$	$\eta=0.1$	$\eta=0.2$	$\eta=0.3$	$\eta=0.4$	$\eta=0.5$
0 ⁺	1.00000	0.92108	0.73218	0.54261	0.39781	0.29611	1.00000	0.92108	0.73218	0.54261	0.39781	0.29611
0.1	1.08000	1.00000	0.79914	0.59343	0.43545	0.32426	1.05331	0.97404	0.78123	0.58337	0.42999	0.32123
0.2	1.32000	1.23677	1.00000	0.74590	0.54836	0.40873	1.20772	1.12325	0.91749	0.69812	0.52197	0.39386
0.3	1.72000	1.63138	1.33477	1.00000	0.73654	0.54951	1.42664	1.33477	1.11273	0.86736	0.66156	0.50658
0.4	2.28000	2.18383	1.80345	1.35575	1.00000	0.74660	1.66005	1.56515	1.33330	1.06688	0.83264	0.64898
0.5	3.00000	2.89413	2.40604	1.81313	1.33873	1.00000	1.87586	1.78326	1.55204	1.27487	1.01913	0.80985

\bar{u}_{\max}/\bar{u}_0												
ζ	$\mathfrak{M} \rightarrow 2/3$						$\mathfrak{M} \rightarrow 1$					
	$\eta=0$	$\eta=0.1$	$\eta=0.2$	$\eta=0.3$	$\eta=0.4$	$\eta=0.5$	$\eta=0$	$\eta=0.1$	$\eta=0.2$	$\eta=0.3$	$\eta=0.4$	$\eta=0.5$
0 ⁺	1.00000	0.92108	0.73218	0.54261	0.39781	0.29611	1.00000	0.92108	0.73218	0.54261	0.39781	0.29611
0.1	1.02655	0.94888	0.76408	0.57365	0.42467	0.31824	1.00000	0.92466	0.74763	0.56424	0.41948	0.31532
0.2	1.09670	1.02277	0.84694	0.65603	0.49799	0.38004	1.00000	0.93691	0.78616	0.61869	0.47611	0.36714
0.3	1.17870	1.11273	0.95158	0.76544	0.60037	0.46986	1.00000	0.95158	0.83053	0.68481	0.54951	0.43809
0.4	1.25031	1.19442	1.05281	0.87863	0.71309	0.57389	1.00000	0.96372	0.86903	0.74660	0.62349	0.51436
0.5	1.30603	1.25984	1.13887	0.98157	0.82237	0.68038	1.00000	0.97261	0.89874	0.79771	0.68919	0.58656

Table 2 Normalized mid-span axial deformation of a mixture unified gradient elastic nanobar with fixed-free ends

$\bar{u}_{\bar{x}=1/2}/\bar{u}_0$												
ζ	$\mathfrak{M} \rightarrow 0$						$\mathfrak{M} \rightarrow 1/3$					
	$\eta=0$	$\eta=0.1$	$\eta=0.2$	$\eta=0.3$	$\eta=0.4$	$\eta=0.5$	$\eta=0$	$\eta=0.1$	$\eta=0.2$	$\eta=0.3$	$\eta=0.4$	$\eta=0.5$
0 ⁺	1.00000	0.97369	0.91073	0.84754	0.79927	0.76537	1.00000	0.97369	0.91073	0.84754	0.79927	0.76537
0.1	1.02667	1.00000	0.93305	0.86448	0.81182	0.77476	1.01777	0.99135	0.92708	0.86112	0.81000	0.77374
0.2	1.10667	1.07892	1.00000	0.91530	0.84945	0.80291	1.06924	1.04108	0.97250	0.89937	0.84066	0.79795
0.3	1.24000	1.21046	1.11159	1.00000	0.91218	0.84984	1.14221	1.11159	1.03758	0.95579	0.88719	0.83553
0.4	1.42667	1.39461	1.26782	1.11858	1.00000	0.91553	1.22002	1.18838	1.11110	1.02229	0.94421	0.88299
0.5	1.66667	1.63138	1.46868	1.27104	1.11291	1.00000	1.29195	1.26109	1.18401	1.09162	1.00638	0.93662

$\bar{u}_{\bar{x}=1/2}/\bar{u}_0$												
ζ	$\mathfrak{M} \rightarrow 2/3$						$\mathfrak{M} \rightarrow 1$					
	$\eta=0$	$\eta=0.1$	$\eta=0.2$	$\eta=0.3$	$\eta=0.4$	$\eta=0.5$	$\eta=0$	$\eta=0.1$	$\eta=0.2$	$\eta=0.3$	$\eta=0.4$	$\eta=0.5$
0 ⁺	1.00000	0.97369	0.91073	0.84754	0.79927	0.76537	1.00000	0.97369	0.91073	0.84754	0.79927	0.76537
0.1	1.00885	0.98296	0.92136	0.85788	0.80822	0.77275	1.00000	0.97489	0.91588	0.85475	0.80649	0.77177
0.2	1.03223	1.00759	0.94898	0.88534	0.83266	0.79335	1.00000	0.97897	0.92872	0.87290	0.82537	0.78905
0.3	1.05957	1.03758	0.98386	0.92181	0.86679	0.82329	1.00000	0.98386	0.94351	0.89494	0.84984	0.81270
0.4	1.08344	1.06481	1.01760	0.95954	0.90436	0.85797	1.00000	0.98791	0.95634	0.91553	0.87450	0.83812
0.5	1.10201	1.08661	1.04629	0.99386	0.94079	0.89346	1.00000	0.99087	0.96625	0.93257	0.89640	0.86219

the nano-sized elastic bar within the framework of the mixture unified gradient theory are endorsed. The axial response of the elastic nanobar is recognized to be less influenced

by the characteristic length-scale parameters for non-vanishing values of the mixture parameter. The size-dependent effects of the gradient characteristic parameters on the

axial deformation of nanobars are more significant for the fixed-end conditions. The axial deformation function of the nano-sized elastic bar coincides with the classical elastic bar model for either vanishing the gradient characteristic parameters, or instead, as the mixture parameter approaches unity in the absence of the strain gradient characteristic parameter.

Numerical values of the normalized axial deformation function at the mid-span of the mixture unified gradient elastic bar, under a uniformly distributed axial load, are, respectively, collected in Tables 1 and 2 for fixed-end and fixed-free boundary conditions. Numerical results of the axial deformation of the nano-sized elastic bar consistent with the mixture unified gradient theory for the prescribed mixture parameter $\mathfrak{M} = 1$ are not depicted in the numerical illustrations, for the sake of clarity, but are tabulated in Tables 1 and 2.

Last but not least, the effectiveness of the mixture unified gradient theory of elasticity in precisely characterizing the nanoscopic features of elastic nanobeams in nonlinear flexure [49] as well as the dynamics of elastic nanobeams is, more recently, evinced in [50, 51].

5 Concluding remarks

The mixture unified gradient theory of elasticity is invoked for an accurate description of the size-dependent structural response of materials at the ultra-small scale. The size-effects of the stress gradient theory and the strain gradient model are consistently integrated with the classical elasticity model within the context of the mixture unified gradient theory. The conceived generalized continuum theory, therefore, addresses a consistent approach to rigorous assessment of nanoscopic field quantities. A stationary variational framework, founded on ad hoc functional space of kinetic source fields, is introduced. The boundary-value problem of the associated equilibrium of the nano-sized elastic bar is established and properly equipped with a complete set of boundary conditions. The explicit formulae of the axial resultant fields, describing the extra non-standard boundary conditions, are determined without the need of implementing the sophisticated equivalence lemma necessary in the counterpart framework of the nonlocal gradient models. The detected constitutive model of the axial resultants, cast as ordinary differential relations, is properly enriched with the strain gradient characteristic length, the stress gradient length-scale parameter, and the mixture parameter. All the governing equations associated with the equilibrated elastic nanobar are integrated into a single functional. Various generalized continuum theories of the gradient type, namely the unified gradient theory, the stress gradient theory, the strain gradient theory, and the mixture stress gradient theory, are recovered by properly driving the characteristic length-scale

parameters. The effectiveness of the established variational framework consistent with the mixture unified gradient theory in addressing the peculiar characteristics of nano-scale structures is put into evidence via a comprehensive analysis of both the elastostatic and elastodynamic structural behaviors of nano-sized elastic bars. The dispersive behavior of axial waves is analytically examined and the closed-form solution of the phase velocity of dispersive waves is derived. Nanoscopic features of the wave dispersion are numerically depicted and thoroughly discussed. The efficacy of the introduced generalized continuum theory in describing the dispersive behaviors of waves with wavelengths at the ultra-small scale is demonstrated in comparison with the counterpart experimental measurements. A practical approach for inverse determination of the characteristic length-scale parameters associated with the generalized continuum mechanics theories is introduced. The elastostatic characteristics of nanobars with kinematic constraints of nano-mechanics interest are, furthermore, studied. The axial deformation of a mixture unified gradient elastic bar is analytically addressed via a viable procedure based on successive integration of differential equations of lower-order. The associated nanoscopic elastostatic features of nano-sized bars with fixed-end and fixed-free boundary conditions are graphically demonstrated and comprehensively commented upon. The expected size-dependent features of the elastostatic axial deformation of the nano-sized bar within the framework of the mixture unified gradient theory are confirmed. A new numerical benchmark is detected for elastostatic and elastodynamic analysis of nano-sized elastic bars. The introduced mixture unified gradient elasticity framework provides a promising methodology to tackle the statics and dynamics of bar-type elements of a wide spectrum of cutting-edge engineering systems.

Funding This research did not receive any specific grant from funding agencies in the public, commercial, or not-for-profit sectors.

Declarations

Conflict of interest The authors declare that they have no known competing financial interests or personal relationships that could have appeared to influence the work reported in this paper.

References

1. K. You, C. Li, D. Zhou, B. Kedong, A piezoelectrically tunable resonator based on carbon and boron nitride coaxial heteronanotubes. *Appl. Phys. A* **128**, 667 (2022). <https://doi.org/10.1007/s00339-022-05794-5>
2. A. Karabatak, F. Danişman-Kalındemirtaş, E. Tan, E.-K. Serap, K. Selcan, Kappa carrageenan/PEG-CuO nanoparticles as a multifunctional nanoplatfrom: digital colorimetric biosensor and

- anticancer drug nanocarrier. *Appl. Phys. A* **128**, 661 (2022). <https://doi.org/10.1007/s00339-022-05802-8>
3. M. Rigi Jangjoo, M. Berahman, Room-temperature nitrogen dioxide gas sensor based on graphene oxide nanoribbons decorated with MoS₂ nanospheres. *Appl. Phys. A* **128**, 523 (2022). <https://doi.org/10.1007/s00339-022-05605-x>
 4. K. de Oliveira Gonçalves, F.R.O. Silva, L.C. Courrol, Low-cost hydrogen peroxide sensor based on the dual fluorescence of *Plinia cauliflora* silver nanoparticles. *Appl. Phys. A* **128**, 692 (2022). <https://doi.org/10.1007/s00339-022-05821-5>
 5. I. Elishakoff, D. Pentaras, K. Dujat, C. Versaci, G. Muscolino, J. Storch, S. Bucas, N. Challamel, T. Natsuki, Y.Y. Zhang, C.M. Wang, G. Ghyselinck, *Carbon nanotubes and nano sensors: vibrations, buckling, and ballistic impact* (ISTE-Wiley, London, 2012)
 6. E.C. Aifantis, On the role of gradients in the localization of deformation and fracture. *Int. J. Eng. Sci.* **30**, 1279–1299 (1992). [https://doi.org/10.1016/0020-7225\(92\)90141-3](https://doi.org/10.1016/0020-7225(92)90141-3)
 7. C. Polizzotto, Gradient elasticity and nonstandard boundary conditions. *Int. J. Solids Struct.* **40**, 7399–7423 (2003). <https://doi.org/10.1016/j.ijsolstr.2003.06.001>
 8. S. Forest, K. Sab, Stress gradient continuum theory. *Mech. Res. Commun.* **40**, 16–25 (2012). <https://doi.org/10.1016/j.mechrescom.2011.12.002>
 9. C. Polizzotto, Variational formulations and extra boundary conditions within stress gradient elasticity theory with extensions to beam and plate models. *Int. J. Solids Struct.* **80**, 405–419 (2016). <https://doi.org/10.1016/j.ijsolstr.2015.09.015>
 10. S. Fattaheian Dehkordi, Y. Tadi Beni, Size-dependent continuum-based model of a truncated flexoelectric/flexomagnetic functionally graded conical nano/microshells. *Appl. Phys. A* **128**, 320 (2022). <https://doi.org/10.1007/s00339-022-05386-3>
 11. A. Ashrafi Dehkordi, R. Jahanbazi Goojani, Y. Tadi Beni, Porous flexoelectric cylindrical nanoshell based on the non-classical continuum theory. *Appl. Phys. A* **128**, 478 (2022). <https://doi.org/10.1007/s00339-022-05584-z>
 12. R. Tiwari, R. Kumar, A.E. Abouelregal, Thermoelastic vibrations of nano-beam with varying axial load and ramp type heating under the purview of Moore–Gibson–Thompson generalized theory of thermoelasticity. *Appl. Phys. A* **128**, 160 (2022). <https://doi.org/10.1007/s00339-022-05287-5>
 13. M. Ramezani, M. Rezaiee-Pajand, F. Tornabene, Linear and nonlinear mechanical responses of FG-GPLRC plates using a novel strain-based formulation of modified FSDT theory. *Int. J. Non. Linear Mech.* **140**, 103923 (2022). <https://doi.org/10.1016/j.ijnonlinmec.2022.103923>
 14. J.R. Banerjee, S.O. Papkov, T.P. Vo, I. Elishakoff, Dynamic stiffness formulation for a micro beam using Timoshenko-Ehrenfest and modified couple stress theories with applications. *J. Vib. Control.* (2021). <https://doi.org/10.1177/10775463211048272>
 15. S.K. Jena, S. Chakraverty, V. Mahesh, D. Harursampath, Application of Haar wavelet discretization and differential quadrature methods for free vibration of functionally graded micro-beam with porosity using modified couple stress theory. *Eng. Anal. Boundary Elem.* **140**, 167–185 (2022). <https://doi.org/10.1016/j.engabound.2022.04.009>
 16. A.C. Eringen, *Nonlocal Continuum Field Theories* (Springer, New York, 2002). <https://doi.org/10.1007/b97697>
 17. A.E. Abouelregal, B. Akgöz, Ö. Civalek, Nonlocal thermoelastic vibration of a solid medium subjected to a pulsed heat flux via Caputo-Fabrizio fractional derivative heat conduction. *Appl. Phys. A* **128**, 660 (2022). <https://doi.org/10.1007/s00339-022-05786-5>
 18. X. Yan, Free vibration analysis of a rotating nanobeam using integral form of Eringen's nonlocal theory and element-free Galerkin method. *Appl. Phys. A* **128**, 641 (2022). <https://doi.org/10.1007/s00339-022-05714-7>
 19. H.M. Shodja, H. Moosavian, Weakly nonlocal micromorphic elasticity for diamond structures vis-à-vis lattice dynamics. *Mech. Mater.* **147**, 103365 (2020). <https://doi.org/10.1016/j.mechmat.2020.103365>
 20. H.M. Numanoglu, H. Ersoy, Ö. Civalek, A.J.M. Ferreira, Derivation of nonlocal FEM formulation for thermo-elastic Timoshenko beams on elastic matrix. *Compos. Struct.* **273**, 114292 (2021). <https://doi.org/10.1016/j.compstruct.2021.114292>
 21. A.A. Pisano, P. Fuschi, C. Polizzotto, Integral and differential approaches to Eringen's nonlocal elasticity models accounting for boundary effects with applications to beams in bending. *ZAMM J. Appl. Math. Mech.* **101**, 202000152 (2021). <https://doi.org/10.1002/zamm.202000152>
 22. Ö. Civalek, B. Uzun, M.Ö. Yaylı, B. Akgöz, Size-dependent transverse and longitudinal vibrations of embedded carbon and silica carbide nanotubes by nonlocal finite element method. *Eur. Phys. J. Plus* **135**, 381 (2020). <https://doi.org/10.1140/epjp/s13360-020-00385-w>
 23. I. Elishakoff, A. Ajenjo, D. Livshits, Generalization of Eringen's result for random response of a beam on elastic foundation. *Eur. J. Mech. A Solids* **81**, 103931 (2020). <https://doi.org/10.1016/j.euromechsol.2019.103931>
 24. A.C. Aifantis, On the gradient approach—relation to Eringen's nonlocal theory. *Int. J. Eng. Sci.* **49**, 1367–1377 (2011). <https://doi.org/10.1016/j.ijengsci.2011.03.016>
 25. A.C. Aifantis, Update on a class of gradient theories. *Mech. Mater.* **35**, 259–280 (2003). [https://doi.org/10.1016/S0167-6636\(02\)00278-8](https://doi.org/10.1016/S0167-6636(02)00278-8)
 26. S.A. Faghidian, Flexure mechanics of nonlocal modified gradient nanobeams. *J. Comput. Des. Eng.* **8**, 949–959 (2021). <https://doi.org/10.1093/jcde/qwab027>
 27. S.A. Faghidian, Contribution of nonlocal integral elasticity to modified strain gradient theory. *Eur. Phys. J. Plus* **136**, 559 (2021). <https://doi.org/10.1140/epjp/s13360-021-01520-x>
 28. S.A. Faghidian, K.K. Żur, J.N. Reddy, A mixed variational framework for higher-order unified gradient elasticity. *Int. J. Eng. Sci.* **170**, 103603 (2022). <https://doi.org/10.1016/j.ijengsci.2021.103603>
 29. S.A. Faghidian, Two-phase local/nonlocal gradient mechanics of elastic torsion. *Math. Methods Appl. Sci.* (2020). <https://doi.org/10.1002/mma.6877>
 30. S.A. Faghidian, Higher-order mixture nonlocal gradient theory of wave propagation. *Math. Methods Appl. Sci.* (2020). <https://doi.org/10.1002/mma.6885>
 31. X.W. Zhu, L. Li, Three-dimensionally nonlocal tensile nanobars incorporating surface effect: a self-consistent variational and well-posed model. *Sci. China Technol. Sci.* **64**, 2495–2508 (2021). <https://doi.org/10.1007/s11431-021-1822-0>
 32. Y. Jiang, L. Li, Y. Hu, A nonlocal surface theory for surface–bulk interactions and its application to mechanics of nanobeams. *Int. J. Eng. Sci.* **172**, 103624 (2022). <https://doi.org/10.1016/j.ijengsci.2022.103624>
 33. S.A. Faghidian, K.K. Żur, E. Pan, J. Kim, On the analytical and meshless numerical approaches to mixture stress gradient functionally graded nano-bar in tension. *Eng. Anal. Boundary Elem.* **134**, 571–580 (2022). <https://doi.org/10.1016/j.engabound.2021.11.010>
 34. S.K. Jena, S. Chakraverty, V. Mahesh, D. Harursampath, Wavelet-based techniques for Hygro-Magneto-Thermo vibration of nonlocal strain gradient nanobeam resting on Winkler-Pasternak elastic foundation. *Eng. Anal. Boundary Elem.* **140**, 494–506 (2022). <https://doi.org/10.1016/j.engabound.2022.04.037>

35. G.T. Monaco, N. Fantuzzi, F. Fabbrocino, R. Luciano, Hygro-thermal vibrations and buckling of laminated nanoplates via nonlocal strain gradient theory. *Compos. Struct.* **262**, 113337 (2021). <https://doi.org/10.1016/j.compstruct.2020.113337>
36. G.T. Monaco, N. Fantuzzi, F. Fabbrocino, R. Luciano, Trigonometric solution for the bending analysis of magneto-electro-elastic strain gradient nonlocal nanoplates in hygro-thermal environment. *Math.* **9**, 567 (2021). <https://doi.org/10.3390/math9050567>
37. W. Xiao, L. Li, M. Wang, Propagation of in-plane wave in viscoelastic monolayer graphene via nonlocal strain gradient theory. *Appl. Phys. A* **123**, 388 (2017). <https://doi.org/10.1007/s00339-017-1007-1>
38. S.K. Jena, S. Chakraverty, M. Malikan, H. Mohammad-Sedighi, Hygro-magnetic vibration of the single-walled carbon nanotube with nonlinear temperature distribution based on a modified beam theory and nonlocal strain gradient model. *Int. J. Appl. Mech.* **12**, 2050054 (2020). <https://doi.org/10.1142/S1758825120500544>
39. H.M. Sedighi, M. Malikan, A. Valipour, K.K. Żur, Nonlocal vibration of carbon/boron-nitride nano-hetero-structure in thermal and magnetic fields by means of nonlinear finite element method. *J. Comput. Des. Eng.* **7**, 591–602 (2020). <https://doi.org/10.1093/jcde/qwaa041>
40. A.E. Abouelregal, H.M. Sedighi, A new insight into the interaction of thermoelasticity with mass diffusion for a half-space in the context of Moore–Gibson–Thompson thermodiffusion theory. *Appl. Phys. A* **127**, 1–4 (2021). <https://doi.org/10.1007/s00339-021-04725-0>
41. R. Barretta, S.A. Faghidian, F. Marotti de Sciarra, Aifantis versus Lam strain gradient models of Bishop elastic rods. *Acta. Mech.* **230**, 2799–2812 (2019). <https://doi.org/10.1007/s00707-019-02431-w>
42. S.A. Faghidian, K.K. Żur, J.N. Reddy, A.J.M. Ferreira, On the wave dispersion in functionally graded porous Timoshenko-Ehrenfest nanobeams based on the higher-order nonlocal gradient elasticity. *Compos. Struct.* **279**, 114819 (2022). <https://doi.org/10.1016/j.compstruct.2021.114819>
43. W. Cochran, *The dynamics of atoms in crystals* (Edward Arnold, London, 1973)
44. X. Zhu, L. Li, Longitudinal and torsional vibrations of size-dependent rods via nonlocal integral elasticity. *Int. J. Mech. Sci.* **133**, 639–650 (2017). <https://doi.org/10.1016/j.ijmecsci.2017.09.030>
45. S.A. Faghidian, Analytical inverse solution of eigenstrains and residual fields in autofrettaged thick-walled tubes. *ASME J. Pressure Vessel. Technol.* **139**, 031205 (2017). <https://doi.org/10.1115/1.4034675>
46. S.A. Faghidian, Analytical approach for inverse reconstruction of eigenstrains and residual stresses in autofrettaged spherical pressure vessels. *ASME J. Pressure Vessel. Technol.* **139**, 041202 (2017). <https://doi.org/10.1115/1.4035980>
47. M.A. Caprio, LevelScheme: a level scheme drawing and scientific figure preparation system for Mathematica. *Comput. Phys. Commun.* **171**, 107–118 (2005). <https://doi.org/10.1016/j.cpc.2005.04.010>
48. K.K. Żur, S.A. Faghidian, Analytical and meshless numerical approaches to unified gradient elasticity theory. *Eng. Anal. Boundary Elem.* **130**, 238–248 (2021). <https://doi.org/10.1016/j.enganabound.2021.05.022>
49. S.A. Faghidian, K.K. Żur, I. Elishakoff, Nonlinear flexure mechanics of mixture unified gradient nanobeams. *Commun. Nonlinear Sci. Numer. Simul.* (2022). <https://doi.org/10.1016/j.cnsns.2022.106928>
50. S.A. Faghidian, I. Elishakoff, Wave propagation in Timoshenko-Ehrenfest nanobeam: a mixture unified gradient theory. *ASME J. Vib. Acoust.* (2022). <https://doi.org/10.1115/1.4055805>
51. S.A. Faghidian, A. Tounsi, Dynamic characteristics of mixture unified gradient elastic nanobeams. *Facta Universitatis ser. Mech. Eng.* (2022). <https://doi.org/10.22190/FUME220703035F>

Publisher's Note Springer Nature remains neutral with regard to jurisdictional claims in published maps and institutional affiliations.

Springer Nature or its licensor (e.g. a society or other partner) holds exclusive rights to this article under a publishing agreement with the author(s) or other rightsholder(s); author self-archiving of the accepted manuscript version of this article is solely governed by the terms of such publishing agreement and applicable law.